Supporting Information

A strategy for massively suppressing the shuttle effect in rechargeable Al-Te battery

Xuefeng Zhang, Jiguo Tu,* Mingyong Wang, Shuqiang Jiao*

State Key Laboratory of Advanced Metallurgy, University of Science and Technology Beijing, Beijing 100083, P. R. China.

*E-mail: guo15@126.com (J. Tu), sjiao@ustb.edu.cn (S. Jiao)

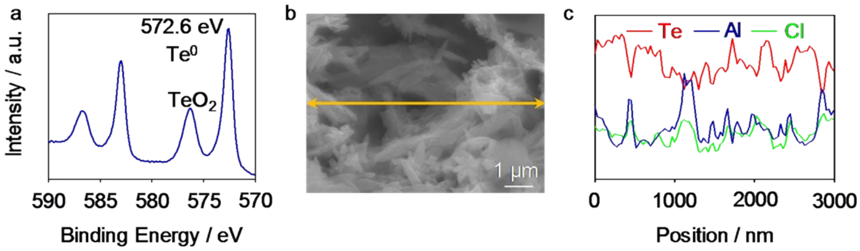

Fig. S1. The characteristic of chemical reaction product. (a) XRD pattern; (b) The SEM image with (c) linear-scanning EDS.

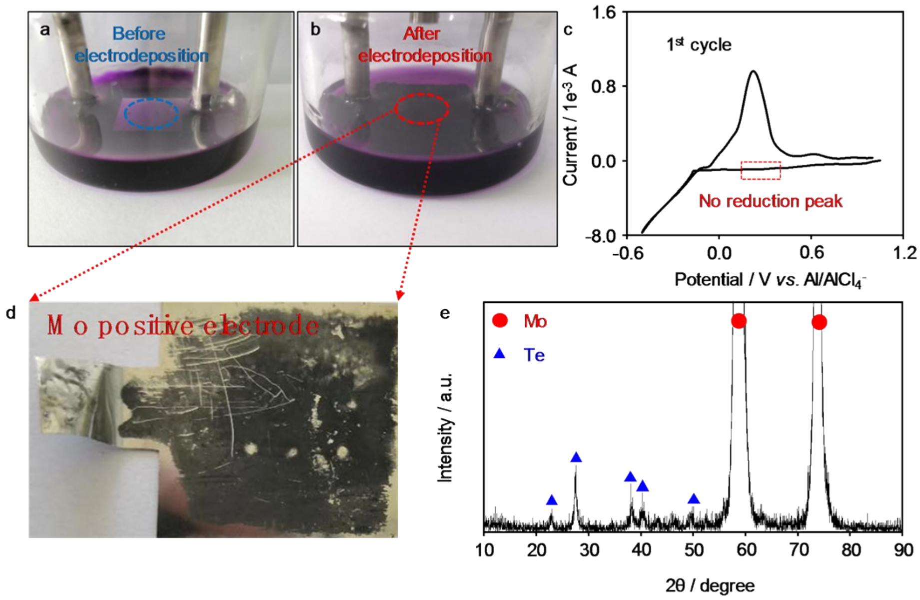

Fig. S2. The electrochemical behavior measurement of soluble ions and the characteristic of electrodeposition product. (a,b) The bottled battery assembled with dissolved electrolyte, Al negative electrode and Mo positive electrode; (c)The first cycle of CVs at voltage range of -0.5 V-1.0 V; (d,e) The photo and XRD pattern of Mo positive electrode after electrodeposition.

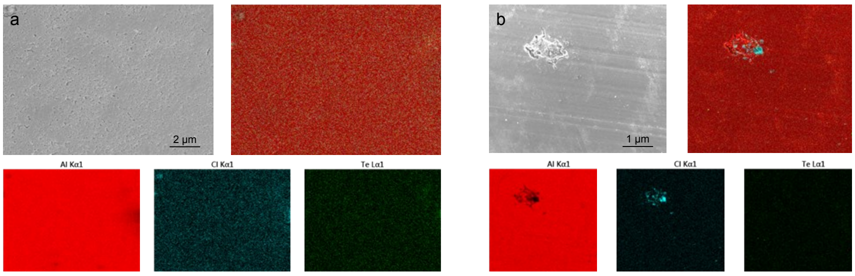

Fig. S3. The SEM images with EDS of Al negative electrode after long cycling. (a) Al│GF/A│Te, (b) Al│AB-PVDF-MS│Te.

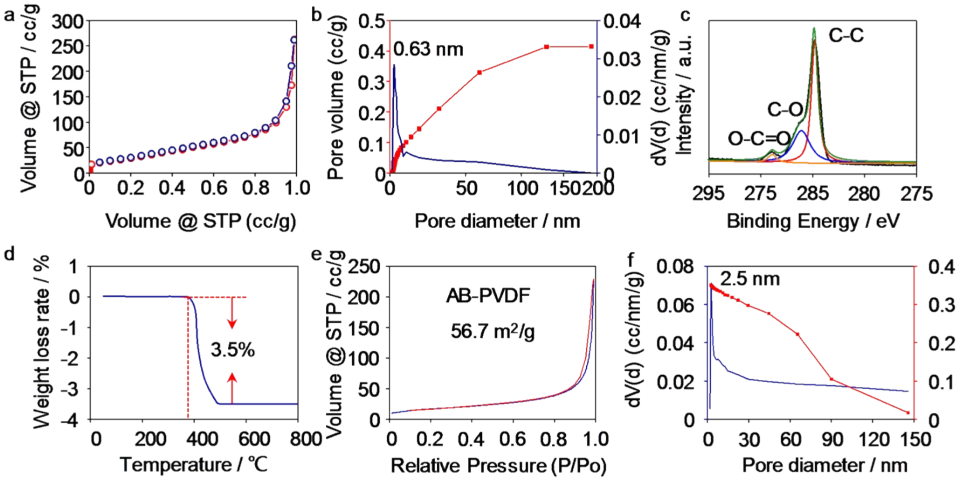

Fig. S4. The characterization of AB and AB-PVDF. (a,b) the BET measurement and corresponding pore size distribution of acetylene black (AB); (c) the XPS spectrum of AB; (d) TGA was carried out under nitrogen operated at a heating rate of 5 °C min^{-1}; (e,f) the BET measurement and corresponding pore size distribution of AB-PVDF.

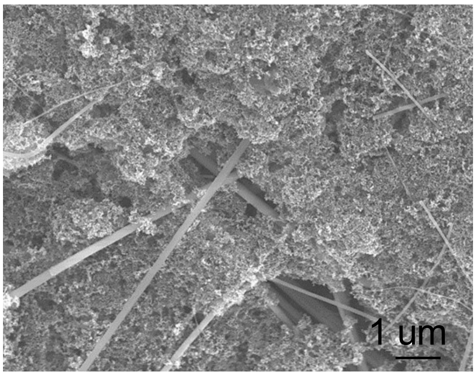

Fig. S5. The SEM image of Acetylene black modified separator (AB-MS) after long-term charge/discharge cycling.

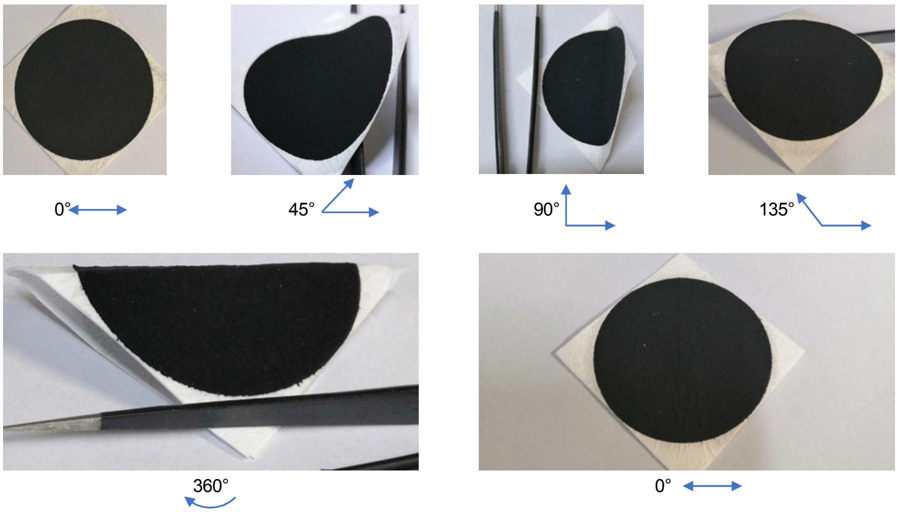

Fig. S6. The Digital photos of AB-PVDF-MS was folded at different angles.

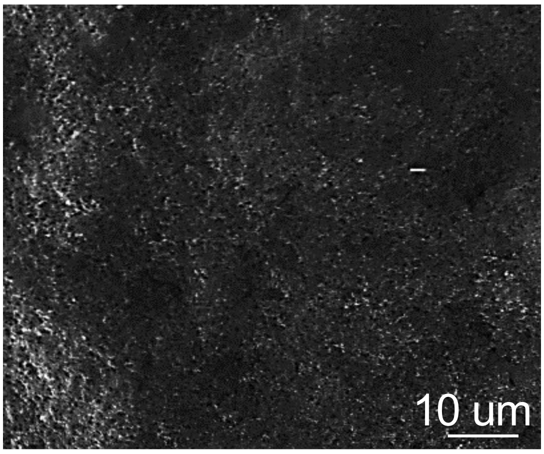

Fig. S7. The SEM image of AB-PVDF-MS from a top view.

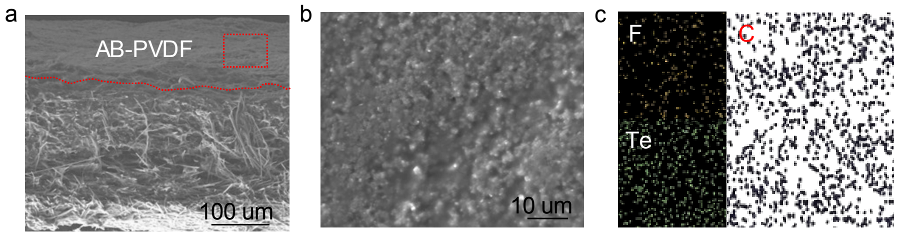

Fig. S8. The SEM and EDS images of AB-PVDF-MS after long-term cycling.

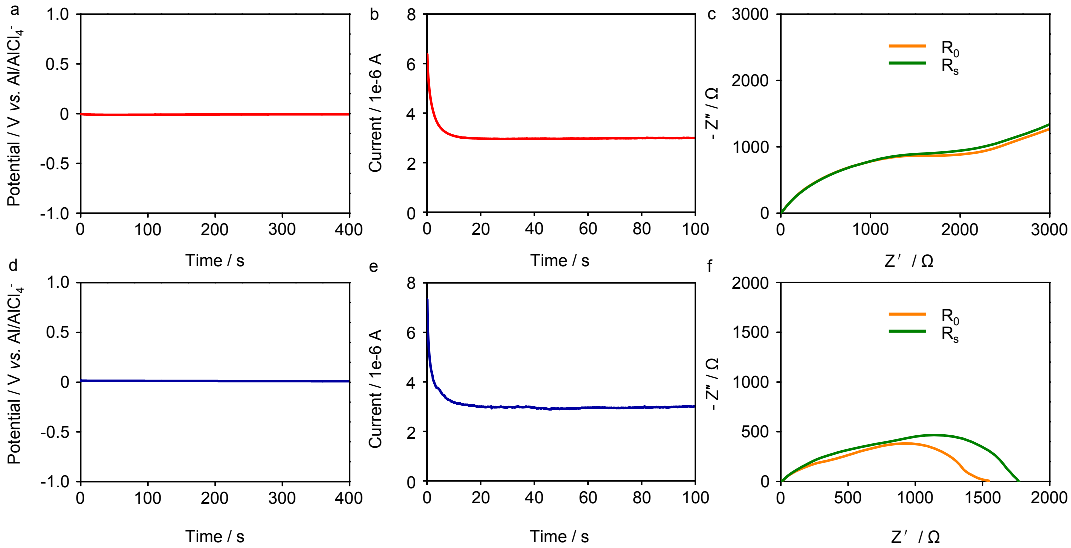

Fig. S9. The transference number (t_{anion}) of conventional separator and AB-PVDF-MS. (a-c) open circuit potential, polarization curve and electrochemical impedance spectra; (d-f) the corresponding measurements for AB-PVDF-MS.

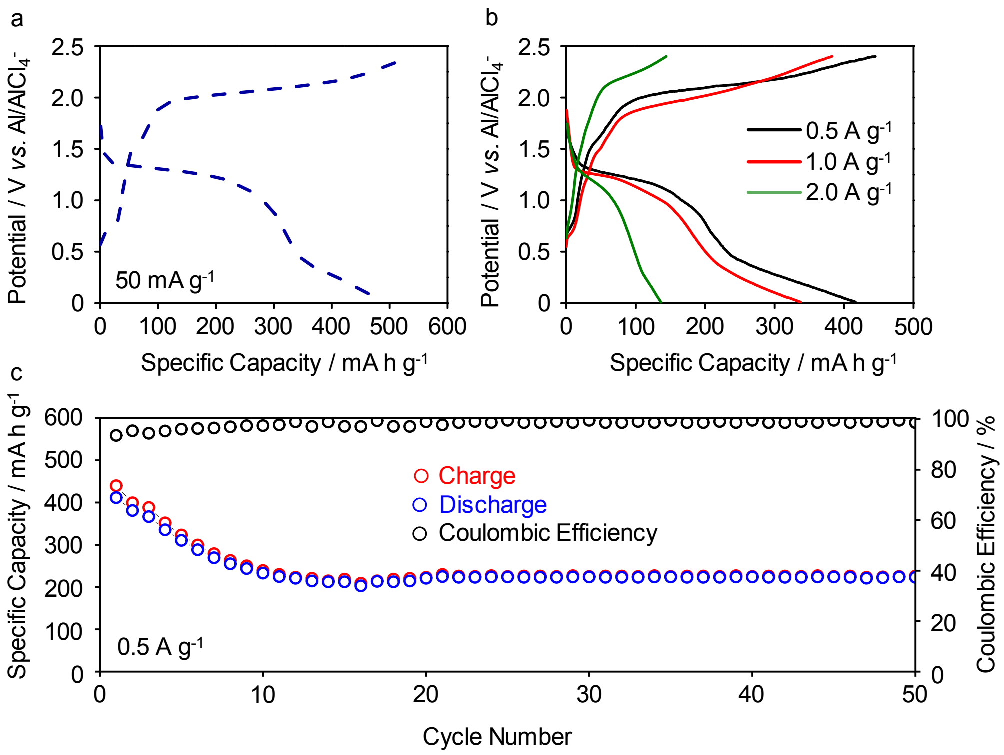

Fig. S10. the electrochemical performance of TABs with conventional separator. (a) the charge/discharge curves at a current density of 50 mA g^{-1}; (b) the charge/discharge curves at different current density; (c) cycling performance at a current density of 0.5 A g^{-1}.

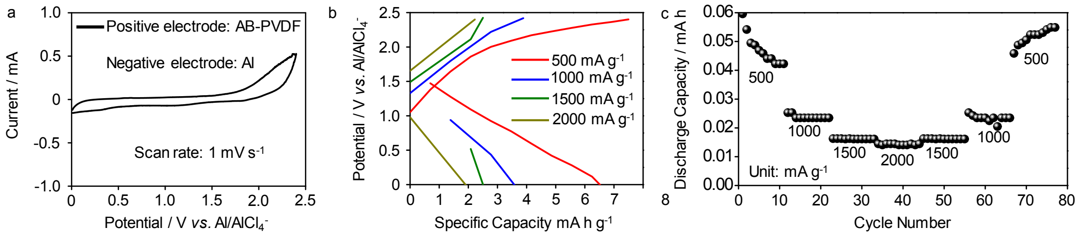

Fig. S11. Electrochemical performance of AB-PVDF. (a) the CVs; (b) The charge/discharge curves at different current density; (c) the rate performance.

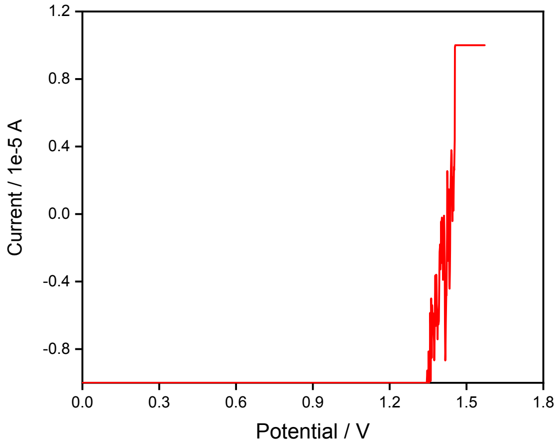

Fig. S12 the LSV curves of AB-PVDF-MS.

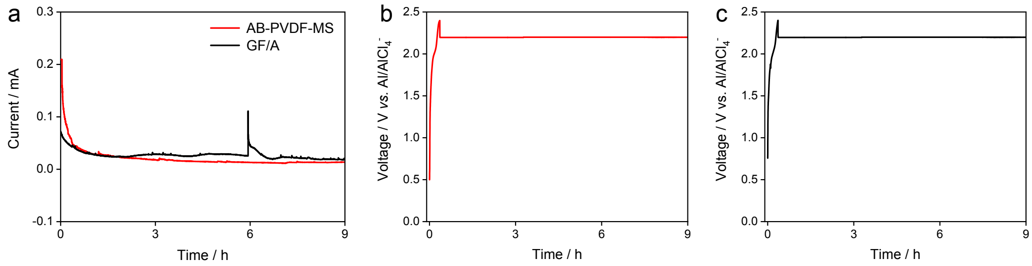

Fig. S13. (a) The self-discharge behaviors of Al|GF/A|Te and Al|AB-PVDF-MS|Te battery system by floating current analysis. (b,c) the corresponding v-t curves.

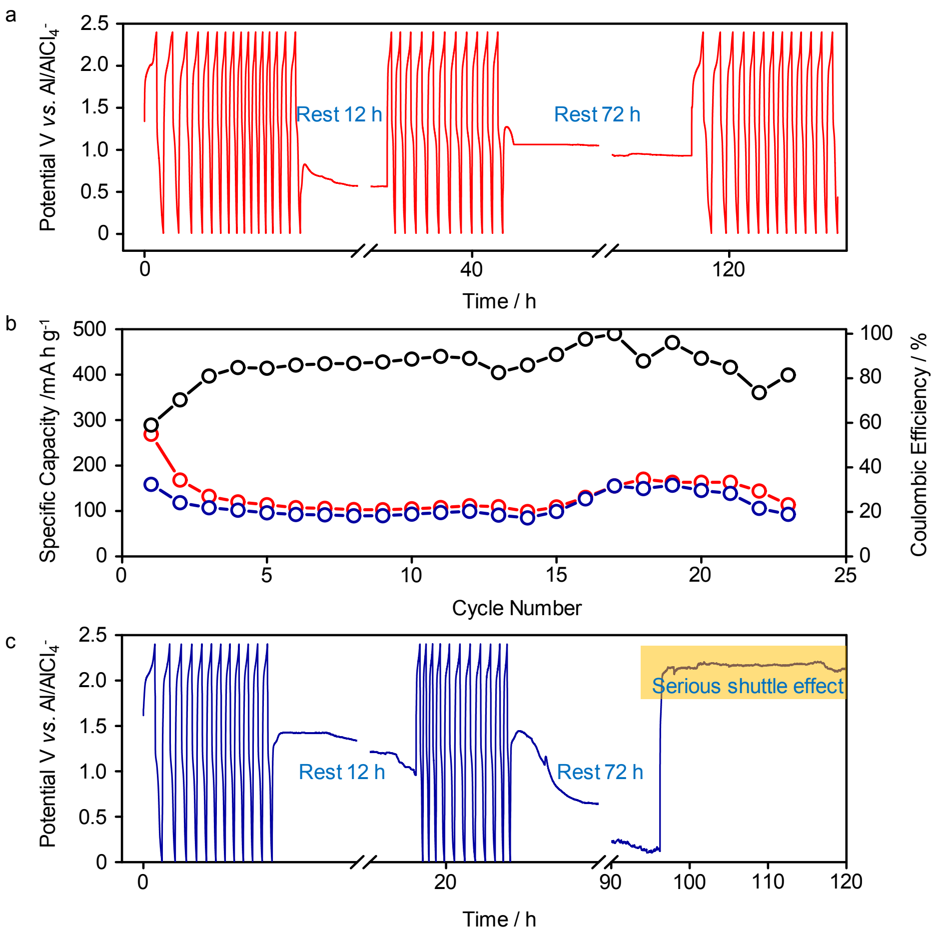

Fig. S14. the cycling performance with different rest time. (a) The potential *vs.* time curves with AB-PVDF-MS; (b,c) the cycling performance and potential *vs.* time curves with conventional separator.

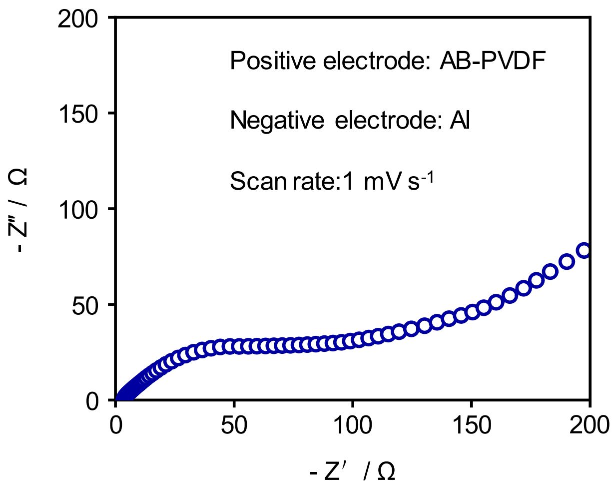

Fig. S15. Electrochemical impedance spectra of AB-PVDF.

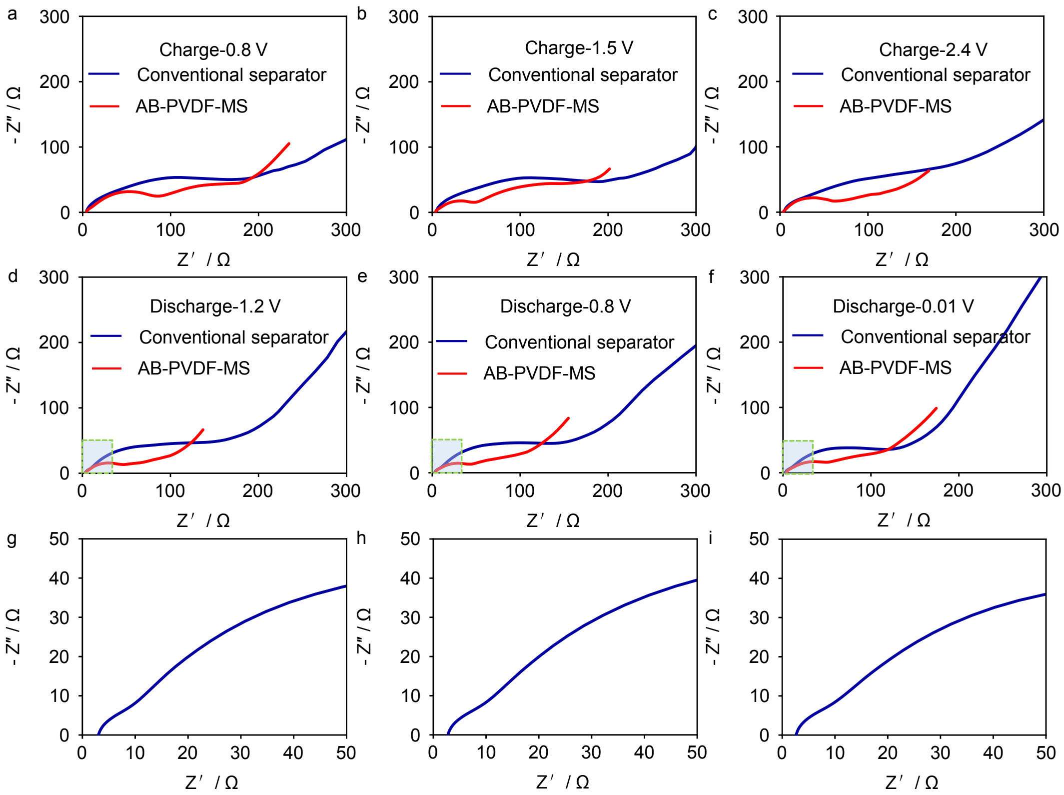

Fig. S16. the electrochemical impedance spectra of the TABs using AB-PVDF-MS, recorded at different potentials of charge and discharge. (a) charge-0.8 V; (b) charge-1.5 V; (c) charge-2.4 V; (d) discharge-1.2 V; (e) discharge-0.8 V and (f) discharge-0.01 V; (g-i) corresponds to a partial enlargement of (d-f).

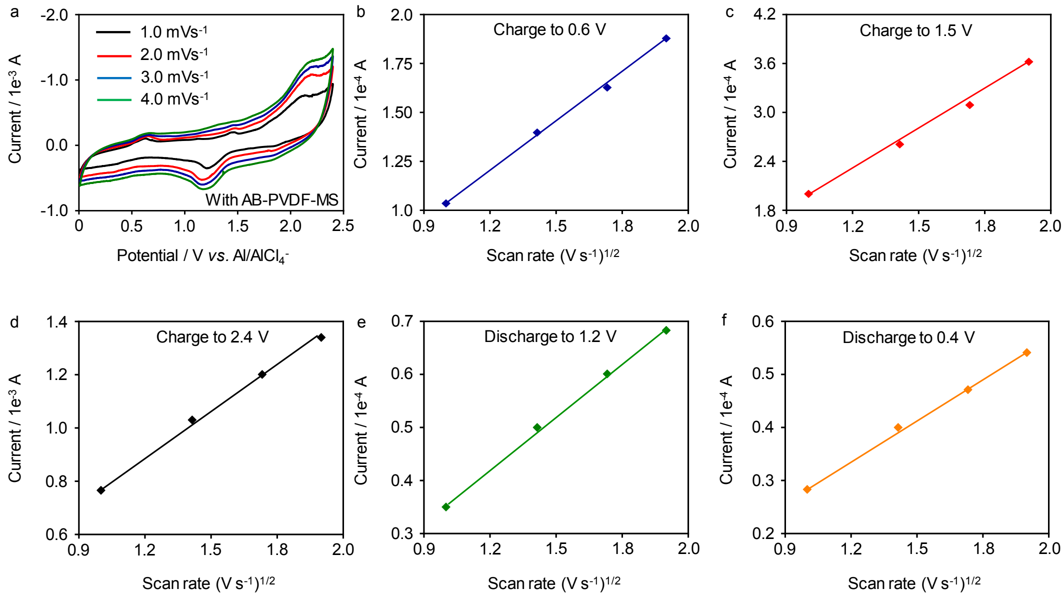

Fig. S17. Cyclic voltammograms at different scan rates of TABs with AB-PVDF-MS and displayed a linear relationship between peak current and scanning rate. (a) The CVs at different scan rate; (b) charge-0.6 V; (c) charge-1.5 V; (d) charge-2.4 V; (e) discharge-1.2 V and (f) discharge-0.4 V.